Finite Element Method Calculations on Statistically Consistent Microstructures of PBX-9501

Eric M. Mas, Bradford E. Clements, and Axinte Ionita, T-1; and Paul D. Peterson, DX-2

We have used data from image analysis to guide us in creating a finite element mesh of PBX-9501. Information about the binder concentration at different length scales taken from micrographs allows us to create a mesh that naturally incorporates inhomogeneities of the microstructure in a manner that is statistically consistent with the observed microstructure. We then apply constitutive models that are consistent with the different binder concentrations and run finite element simulations

Two-dimensional (2-D) micrographs are needed to generate the necessary statistics to use this technique. The images need to be of sufficient magnification to resolve most of the grains but not too magnified as to not include the largest grains.
Figure 1 shows an example of a 50x gray level image of PBX-9501. The image is binarized at a threshold gray level and the percentage of black pixels is found to be 23%. Given the known binder percentage of 9501 we assume that the black pixels are actually 70% HMX crystals too small to resolve with the micrograph.

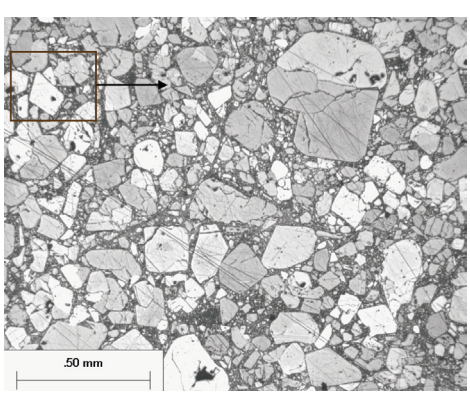

Fig. 1.
A micrograph of PBX-9501.

A complete probability distribution function (PDF) of black pixels can now be determined by successively scanning the image with larger and larger square windows. First 2 pixels by 2 pixels, then 3x3 and so on. The percentage of black pixels in a given window is calculated and the PDF is determined.

To generate a 2-D microstructure we started with a 1024x1024 array of pixels. To be consistent with the image, 23% are black. We now scan the image with a 2x2 pixel window in the same way we did the micrograph. The possible percentages are 0, 25, 50, 75, and 100% black pixels. The probabilities of these percentages are 36, 42, 18, 4, and 0%, respectively, for the randomly generated array, and 65, 7, 9, 10, and 9% for the micrograph. We now calculate the root mean square error (rmse) between the image and generated arrays PDF. Next we randomly switch two pixels, modify the PDF accordingly, and recalculate the rmse. A switch is rejected if the rmse increases. By switching pixels we ensure that the overall ratio of black pixels is preserved. This recipe is followed for 3x3, 2x2, 4x4, 3x3, 2x2 windows and so on until the full PDF is fitted. In Fig. 2 we show the resulting 2-D mesh. We note that the scale is similar to that in Fig. 1. As can be seen in the image we are able to reproduce the various crystal sizes. Also note that the structure is stochastic, so if we started with a different random number seed we would have produced a different but statistically equivalent microstructure.

Creating a 3-D mesh is very similar to creating the 2-D one except instead of a 2-D array we have a 3-D array that we "page through." First we create a 128x128x128 array and randomly populate it. In this case, however, we didn't use the finest scale data. We start with a length scale we can hope to resolve in a simulation, ~ 20 microns or 10 pixels. We now populate

our array with percentages consistent with the micrograph PDF for the 10x10 window. Now, instead of black and white we have gray levels from 0–100 representing the binder percentage for that pixel (element). We now apply our scanning windows for all 128 2-D "pages" of our array. We do this in the three (x, y, and z) directions. This naturally creates 3-D regions that represent individual grains. Note that we are assuming that the composite is isotropic.

Figure 3 illustrates a subset of the 3-D mesh we just described. To use the mesh described here we need a theory that can accommodate different formulations of PBX-9501. Our hybrid Method of Cells / Modified Eshelby-Mori-Tanaka model has this capability [1]. The method hinges on creating a representative volume element of PBX-9501. We use a 2x2x2 RVE with one large subcell representing the large HMX crystals and the other seven subcells use our Modified Eshelby-Mori-Tanaka model [2, 3] or "dirty binder" model to represent small HMX crystals in the polymer matrix. By changing the relative size of the subcells we are able to represent the different binder concentrations in the mesh.

Using the finite element code EPIC [4] to conduct simulations, we applied velocity boundary conditions on the top and bottom nodes in Fig. 3 to approximate a split-Hopkinson pressure bar experiment. The resulting stress strain curve is shown in Fig. 4. Other quantities such as pressure show similar distributions.

By incorporating 2-D image analysis data into a 3-D finite element mesh we are able to represent the fluctuations of fields such as stress and pressure. This information may be invaluable when we investigate ignition that is thought to be driven by local fluctuations in pressure and temperature.

For more information contact Eric Mas at mas@lanl.gov.

[1] B.E. Clements and E.M. Mas, *Modeling Simul. Mater. Sci. Eng.* **12**, 407–421, 2004.
[2] B.E. Clements and E.M. Mas, *J. Appl. Phys.* **90**, 5522–5534, 2002.
[3] E.M. Mas, and B.E. Clements, J. *Appl. Phys.* **90**, 5535–5541, 2002.
[4] G.R. Johnson, et al., "User Instructions of the 1997 Version of the APIC Code," Wright Laboratory, Armament Directorate, Eglin Air Force Base report, WL-TR-1997-7037, 1997.

Funding Acknowledgements
The DoD/DOE Munitions Technology Development Program and NNSA's Advanced Simulation and Computing (ASC) High Explosives Program.

.

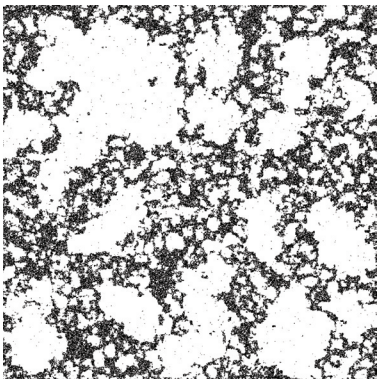

Fig. 2.
The 2-dimensional mesh generated from the statistics taken from the micrograph. The array is 1024x1024 pixels.

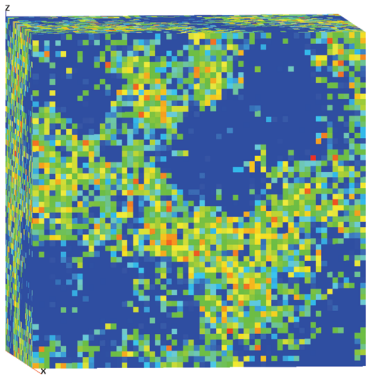

Fig. 3.
A 3-dimensional hexagonal mesh of PBX 9501. The gray levels indicate different percentages of binder.

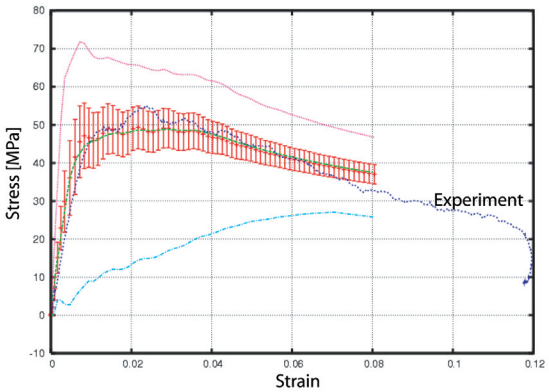

Fig. 4.
Stress-strain curves for PBX 9501. The experimental curve is labeled, the top and bottom curves show the highest and lowest stress in an element at that strain during the simulation, the error bars are one standard deviation above and below the mean and the curve in the middle of those bars is the average stress-strain curve.